SUPPORTING INFORMATION

Table of Contents

A. Nitrogen adsorption and desorption isotherms of SBA-15

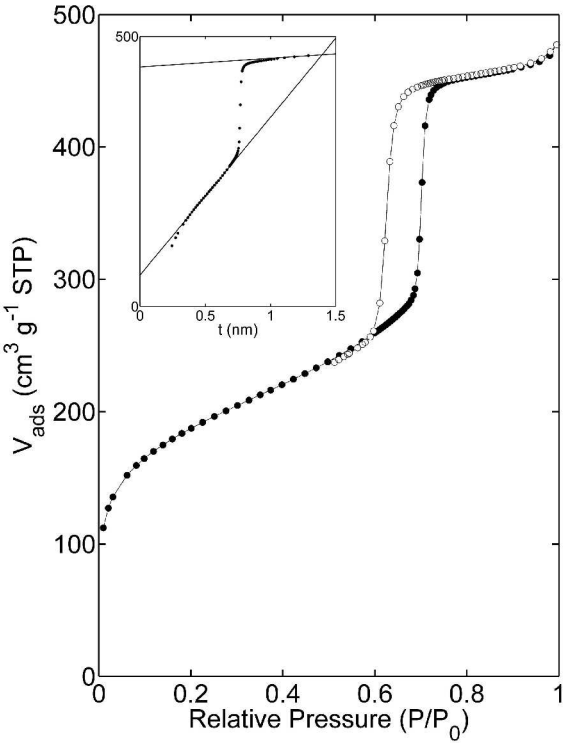


Figure SI-1. Nitrogen adsorption (●) and desorption (○) isotherms of SBA-15. The corresponding t-plot, obtained from the adsorption isotherm with LiChrospher [41, 20] as a standard, is shown in the inset.

## B. Sensitivity of the image analysis to resolution and to noise

The usual approach to image analysis consists in segmenting first the images in order to determine to which phases of the material every pixel belongs, e.g. on the basis of the intensity, and in characterizing afterwards the morphology of the segmented phases. This method cannot be applied to electron tomography reconstruction of beam-sensitive samples; the restriction of the electron dose leads to a low signal over noise ratio, which precludes a reliable segmentation.

The impossibility of segmentation does not, however, rule out quantitative image analysis. The use of an a priori morphological model enables to quantitate noisy images. This is the approach used in the present paper, in which the section of the pores is assumed a priori to be circular. In such a case, the problem of image analysis amounts to the determination of parameters of the model, namely of the pores centers and radii. In this supporting section, we test the robustness to noise of the method used to fit the model. For that purpose, we first proceed to estimate quantitatively the noise over signal ratio of the reconstructions of SBA-15. We then create model images with perfectly cylindrical pores, which we blur to model the finite resolution of the reconstructions, and to which we add Gaussian noise. We finally apply to these model images the analysis method proposed in the main text, to assess the amount of corrugation that may spuriously result from finite resolution and from noise.

Figure SI-2 compares the histograms of grey-tones of a reconstruction of SBA-15 in a volume taken inside the crystallite and in the empty space surrounding the crystallite. In an ideal situation, the latter distribution would contain a single grey-tone corresponding to the void; the former distribution would contain only grey-tones corresponding to the void and to the silica. This is clearly not the case; the breadth of the grey-tone distributions points to the noisiness of the

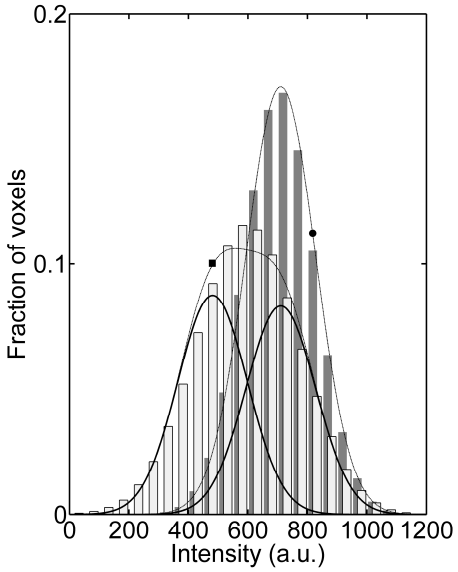


Figure SI-2. Grey-tone intensity distribution of the tomograms corresponding: to the empty space around the SBA-15 crystallite (dark grey), and to the SBA-15 crystallite itself including solid and pore space (bright grey). The lines are fits of the distributions with a Gaussian function (●) and with a sum of two Gaussian functions having the same variance (■).

reconstructions. We assume hereafter that the grey-tone intensity of the reconstruction at any point **x** is given by

$$I(\mathbf{x}) = I_0 + \Delta I\ \Phi(\mathbf{x}) + \sigma_N\ n(\mathbf{x}) \qquad \text{Eq. SI-1}$$

where $I_0$ is the intensity in the silica, $\Delta I$ is the contrast between pore (or void) and silica, and $\Phi(\mathbf{x})$ is an indicator function equal to 0 in the solid, and to 1 outside the crystallite as well as in the pores. The last term in Equation SI-1 models the noise; it has standard deviation $\sigma_N$, and $n(\mathbf{x})$ can be any stochastic function with average 0 and variance 1.

The histogram of grey-tones outside the crystallite (Figure SI-2) is well fitted by a Gaussian distribution with average 710 and standard deviation 117, using a Kolmogorov-Smirnov fitting procedure. From Equation SI-1, this corresponds to $I_0+\Delta I = 710$ and $\sigma_N = 117$, because $\Phi = 1$ everywhere outside the crystallite. Taking this into account, Equation SI-1 predicts that the histogram of grey-tones inside the crystallite be a sum of two Gaussian distributions with the same standard deviation $\sigma_N$, centered on $I_0+\Delta I$ and $I_0$ respectively, and with amplitudes $\langle\Phi\rangle$

and 1-<Φ>. In the last sentence, the brackets denote the spatial average, so that <Φ> is the porosity. The Kolmogorov-Smirnov fit of the histogram with only $\Delta I$ and <Φ> as free parameters leads to $I_0 = 481$, $\Delta I = 229$, and <Φ> = 0.49. From these values, the noise over signal ratio of the reconstruction of SBA-15 is estimated as $\sigma_N/\Delta I = 0.51$.

Figure SI-3 shows the model images we use to assess the impact of both finite resolution and noise on the output of image analysis. Figure SI-3a is an array of cylindrical pores with radius 3 nm, positioned on a hexagonal lattice with spacing 11 nm; the intensity is 481 in the silica and 710 in the pores. The point spread function of the reconstruction is modeled as a Gaussian kernel with standard deviation 2 nm, in agreement with the estimated resolution of the actual reconstruction of SBA-15. Figure SI-3b is obtained by convoluting the initial image with the Gaussian point spread function. Finally, Gaussian noise with standard deviation $\sigma_N$ =117 is added to the convoluted image. The final image in Figure SI-3c is a realistic model of how perfectly cylindrical pores would be imaged with the setup used to image SBA-15 in the main text.

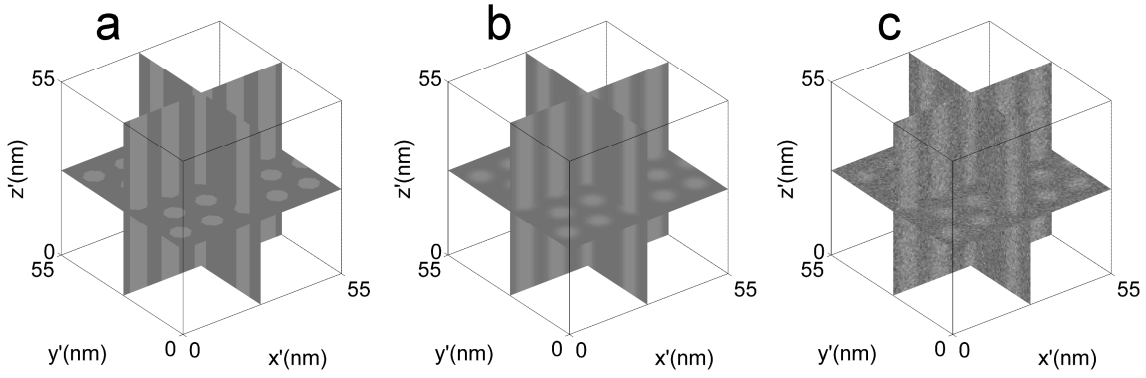


Figure SI-3. Model grey-tone images consisting in (a) cylindrical pores, (b) the same image convoluted with a Gaussian kernel with standard deviation 2 nm to model the finite resolution, and (c) the same convoluted image to which statistical noise is added with a signal over noise ratio equal to 0.5.

The model images in Figure SI-4a and 4b are obtained as in Figure SI-3, with $\sigma_N/\Delta I = 0.5$ and $\sigma_N/\Delta I = 1$, respectively. Note that the level of noise in Figure SI-4b is objectively twice as high as in the reconstructions of SBA-15. These images were analyzed using the same image analysis as used for SBA-15 in the main text, leading to Figures SI-4c and SI-4d. The visual comparison of Figure SI-4c with Figure 5c of the main text shows that the corrugation measured from the reconstruction of SBA-15 does not result from the presence of noise in the images.

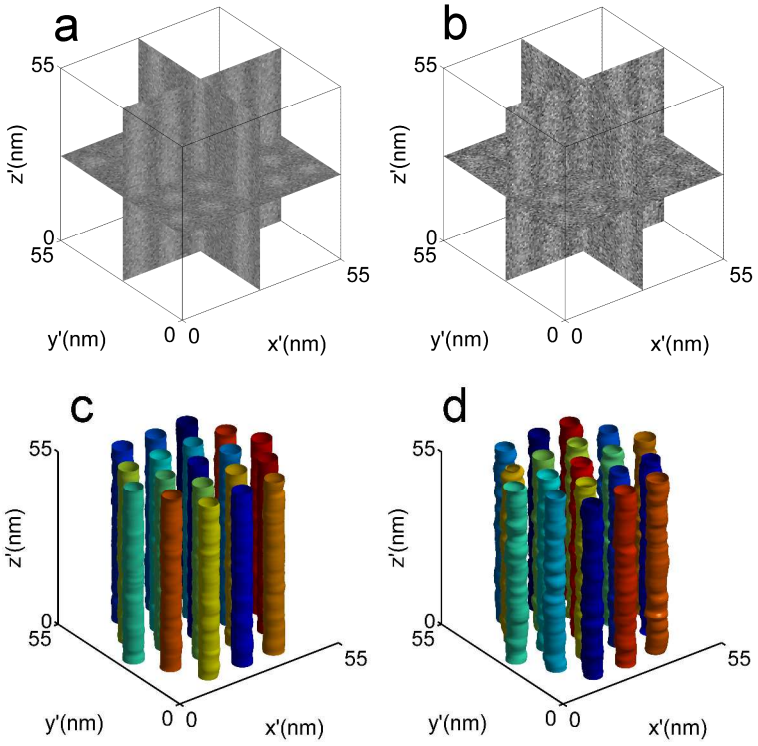


Figure SI-4. Model images of perfect cylinders with a resolution of 2nm to which Gaussian noise was added with amplitude $\sigma_N/\Delta I = 0.5$ (a) and $\sigma_N/\Delta I = 1$ (b); these two model images were analyzed using the same image analysis as in the main text, leading to (c) and (d), respectively. The level of noise in (a) is comparable to that in the actual reconstruction of SBA-15

Figure SI-5 shows the statistical distributions of the deviation between estimated position of the pore centers and the hexagonal lattice $\delta_{xy}$, and of the estimated pore diameters $d$. The fitted values are $\delta_{xy} = 0.0 \pm 0.17$ nm and $d = 5.9 \pm 0.13$ nm for $\sigma_N/\Delta I = 0.5$, and $\delta_{xy} = 0.0 \pm 0.22$ nm and $d = 5.9 \pm 0.26$ nm for $\sigma_N/\Delta I = 1$. When converted to a corona thickness using Equation 3 of the main text, these values lead to $\delta = 0.44$ nm for $\sigma_N/\Delta I = 0.5$, which is four times smaller than the value found for SBA-15. For a level of noise that is twice as high as in the actual reconstruction (assuming $\sigma_N/\Delta I = 1$), one finds $\delta = 0.65$ nm, *i.e.* a corona that is more than two times thinner than in SBA-15.

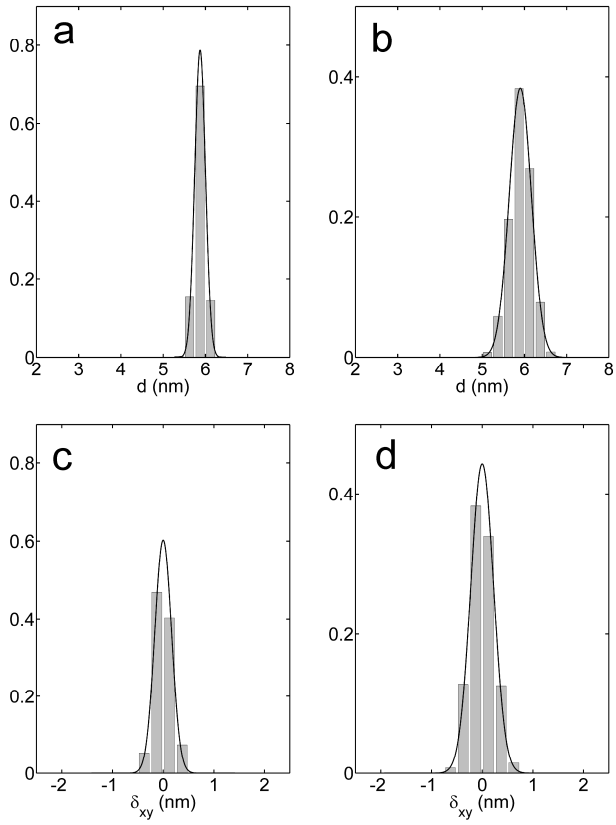


Figure SI-5. Distributions of the local pore diameter $d$ (a and b), and of the deviation between pore centers and points of the hexagonal lattice $\delta_{xy}$ (c and d), for the model images of perfect cylinders with a resolution of 2 nm. Figures a and c are for $\sigma_N/\Delta I = 0.5$ and Figures b and d are for $\sigma_N/\Delta I = 1$ (bottom row). Compare this Figure with Figure 6 of the main text.

## C. Fitting of a 2D lattice to the position of the pore centers

The image analysis procedure provides the height-dependent x' and y' positions of the center of each pore (Figure 4c). In Figure SI-6a, the centers of the pores at a given height are plotted together with the 2D lattice that minimizes the overall distance between the centers and their closest lattice point. This is done for each height z' independently; the obtained two lattice vectors are plotted in Figure SI-6b as a function of height z'. In this figure, it is seen that the array of pores is generally bent and also minimally twisted.

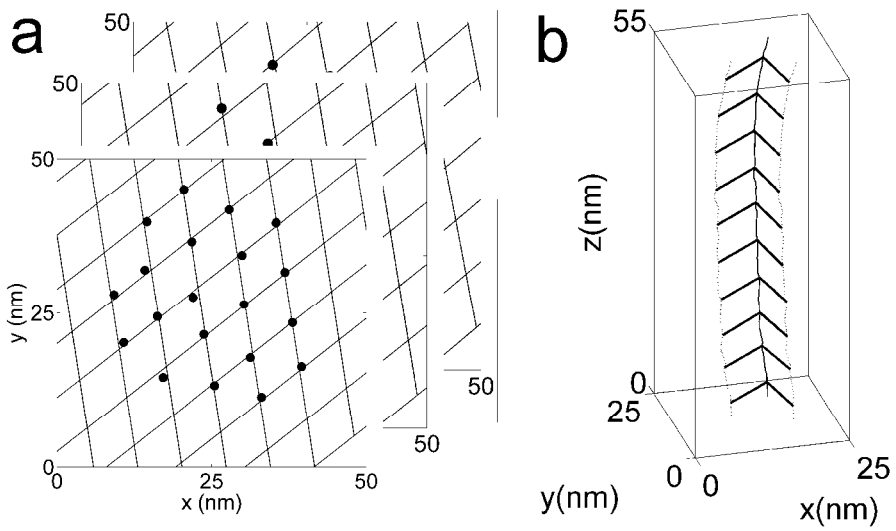


Figure SI-6: z'-dependent crystalline structure of SBA-15: (a) at each height along the pores a 2D lattice is adjusted to the pore centers; the z' dependence of the base vectors (b) shows that the pores are collectively bent and minimally twisted.

For each sample and each z'-slice, the two base vectors are determined independently from one another, and without making any hypothesis on the lattice structure. The average value of the difference in length between the two base vectors is about 2.5% of their average length. According to a test of equal means, however, the difference is not statistically significant with a p-value of $p = 0.17$. This latter value means that there is a probability of more than 17% that a larger difference in length between the two base vectors would be observed given the null hypothesis that the mean lengths of the two base vectors were equal. Figure SI-7a shows the statistical distribution of the pooled lattice spacings; the average spacing is a = 10.3 ± 0.3 nm. Figure SI-7b is the distribution of the angle between the two base vectors. The average angle is 60.6°, which is not statistically different from 60° according to a test of equal means ($p = 0.22$).

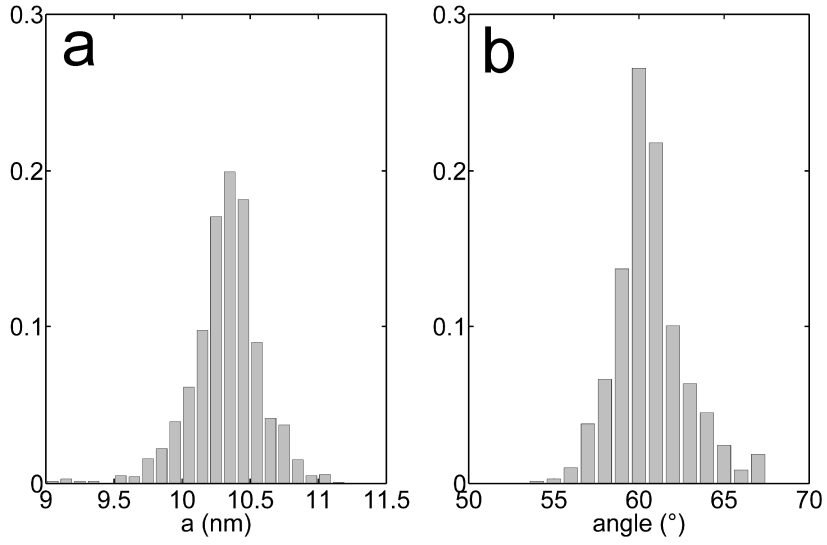


Figure SI-7: Distribution of lattice spacing (a) and of angle between bases vectors (b), determined from image analysis.

## D. Correlation of $\delta_{xy}$ and of $d$ along a given pore

The deviation between pore centers and the vertices of a 2D hexagonal lattice are Gaussian random variables that are correlated along any given pore. To quantitate the correlation, the correlation function $C_{xy}(z')$ is calculated as

$$C_{xy}(z') = \frac{\left\langle \left(\delta_{xy}(z+z') - \left\langle \delta_{xy} \right\rangle\right)\left(\delta_{xy}(z) - \left\langle \delta_{xy} \right\rangle\right) \right\rangle}{\left\langle \left(\delta_{xy}(z) - \left\langle \delta_{xy}(z) \right\rangle\right)^2 \right\rangle} \qquad \text{Eq. SI-2}$$

where the brackets denote the average on all possible values of $z$. $C_{xy}(z')$ is the correlation along any given pore between $\delta_{xy}$ in two slices separated by a given distance z'. It is plotted in Figure SI-8a. The deviations are correlated for distances along the pore smaller than about 5nm. At larger distances $C_{xy}$ tends to 0, which points to the fact that the values of $\delta_{xy}$ are not correlated over long distances. The particular value 5 nm can be though of as the length of the zigzags in the pore centerlines.

The correlation function of the diameters is calculated using Equation SI-2, replacing $\delta_{xy}(z)$ by $d(z)$. The local diameters of the pores are also found to be correlated (Figure SI-8b) along a given pore over a distance close to 4-5 nm.

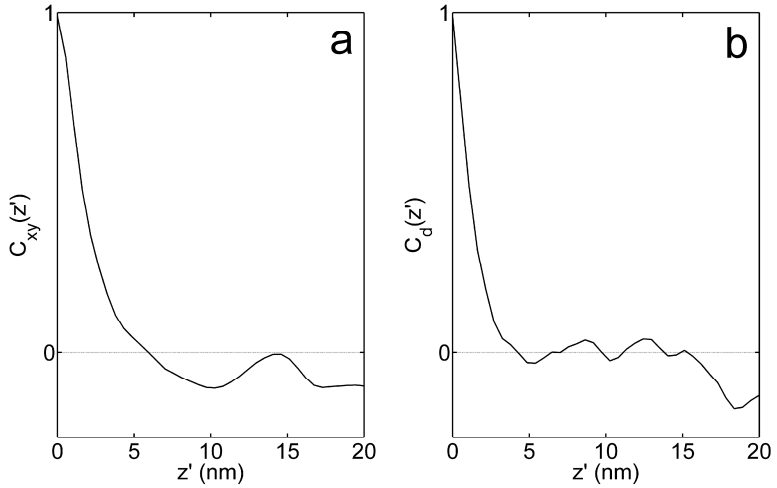


Figure SI-8 Correlation function of $\delta_{xy}$ (a) and of $d$ (b) along any given pore, calculated according to Equation S6-1.

## E. Specific pore volumes determined from the corona model and their comparison with adsorption data

In this section, we first derive the specific pore volumes corresponding to the linear corona model by assuming that the wall is not porous. We then proceed to estimate the porosity of wall that is needed to match the volumes determined by XRD and by physisorption. Using the estimated porosity of the wall, we eventually estimate the pore volume located in the pore center, in the corona, and in the wall.

The figures on which the calculations are based, are taken from section 3.1 of the main text:

- Density of non-porous silica $\rho_{SiO2}$ = 2.2 g cm$^{-3}$;
- XRD: lattice size a =10.8 nm; inner and outer radial limits of the corona $r_i$ = 2.7 nm and $r_o$ = 4.6 nm;
- $N_2$ adsorption: total pore volume $V_{tot}$ = 0.66 cm³/g; of which the mesoporous volume is $V_{meso}$ = 0.57 cm³/g and the microporous volume is $V_{micro}$ = 0.09 cm³/g.

The linear corona model [21] is defined by a dimensionless density profile given by

$$\tilde{\rho}(r) = \begin{cases} 0 & for\ r < r_i \\ (r - r_i)/(r_o - r_i) & for\ r_i < r < r_o \\ 1 & for\ r > r_o \end{cases} \qquad \text{Eq. SI-3}$$

where $r$ is the radial distance from the pore center. The phase with density $\tilde{\rho} = 1$ need not be dense silica and it may be porous. We shall refer to it hereafter as being simply phase m (for matter); the other phase is referred to as phase p (for pore). The use of these general names is

necessary to avoid confusion because pores may be present both in phase p (in the corona) and in phase m (in the pore wall and in the corona).

The total volume of phase m in the unit cell of the hexagonal array, per unit length of the pores, is determined as

$$v_{cell}^{m} = \frac{\sqrt{3}}{2} a^2 - \pi r_o^2 + v_{corona}^{m} \qquad \text{Eq. SI-4}$$

where the first term is the total surface of the hexagonal unit cell, the second term is the surface of the circle containing both the central pore and the corona, and the last term is the amount of matter in the corona. The latter quantity is estimated as

$$v_{corona}^{m} = \int_{r_i}^{r_e} \tilde{\rho}(r)\ 2\pi r\ dr = \frac{\pi}{3}\left[2r_o^2 - r_i\left(r_o + r_i\right)\right] \qquad \text{Eq. SI-5}$$

where the second equality results from the use of Equation SI-3. In the same way, the volume of phase p in the corona is

$$v_{corona}^{p} = \int_{r_i}^{r_e} \left[1 - \tilde{\rho}(r)\right] 2\pi r\ dr = \frac{\pi}{3}\left[r_o^2 + r_i\left(r_o - 2r_i\right)\right] \qquad \text{Eq. SI-6}$$

The total volume of phase p in the unit cell is

$$v_{cell}^{p} = \frac{\sqrt{3}}{2} a^2 - v_{cell}^{m} \qquad \text{Eq. SI-7}$$

Note that Equations SI-4 to SI-7 are volumes per unit length of the pores, so that they are indeed surfaces. Using the figures recalled at the beginning of this section, we find that the total surface of phase p in a unit cell is $v_{cell}^{p}$ = 42.8 nm², of which the surface $v_{corona}^{p}$ = 19.9 nm² is located in the corona. The total surface of phase m is $v_{cell}^{m}$ = 58.2 nm², of which a fraction $v_{corona}^{m}$ = 23.7 nm² is located in the corona region.

Assuming that phase m is dense silica, and using the same notations as in the main text, the total specific pore volume is

$$V_{tot}^{XRD} = \frac{v_{cell}^{p}}{\rho_{SiO2}\ v_{cell}^{m}} \qquad \text{Eq. SI-8}$$

The specific volume of the pores located in the corona is

$$V_{corona}^{XRD} = \frac{v_{corona}^{p}}{\rho_{SiO2}\ v_{cell}^{m}} \qquad \text{Eq. SI-9}$$

and the specific volume corresponding to the central part of the pore (where $r < r_i$) is

$$V_{center}^{XRD} = V_{tot}^{XRD} - V_{corona}^{XRD} \qquad \text{Eq. SI-10}$$

From the values calculated at the end of the previous paragraph, one finds $V_{tot}^{XRD}$ = 0.33 cm³, $V_{corona}^{XRD}$ = 0.16 cm³ g$^{-1}$, and g$^{-1}$, $V_{center}^{XRD}$ = 0.18 cm³ g$^{-1}$. As the total pore volume determined from physisorption is almost the double of $V_{tot}^{XRD}$, one has to assume that the wall is itself porous.

To correct Equations SI-8 to SI-10 in the case where the wall is porous, let us call $\varepsilon$ the volume fraction of pores within phase m. The total specific pore volume is now given by

$$V_{tot} = \frac{v_{cell}^{p} + \varepsilon\ v_{cell}^{m}}{\rho_{SiO2}(1-\varepsilon)\ v_{cell}^{m}} \qquad \text{Eq. SI-11}$$

where the numerator is the sum of the contributions of phase p (pore center and corona) and of phase m (including the part of it in the corona) to the total pore volume; the denominator is the mass of silica in the unit cell with apparent density of phase m written as (1-$\varepsilon$) $\rho_{SiO2}$. Using the value $V_{tot}$ = 0.66 cm³/g taken from physisorption, and the other volumes from XRD, Equation SI-11 predicts $\varepsilon$ = 0.292. This means that physisorption is in agreement with the corona model if the pore wall has a porosity of about 30%.

The specific volume corresponding to the central part of the pore (for $r < r_i$) is calculated as

$$V_{center}^{XRD} = \frac{\pi\, r_i^2}{\rho_{SiO2}(1-\varepsilon)\, v_{cell}^m} \qquad \text{Eq. SI-12}$$

and the phase p of the corona contributes to specific volume

$$V_{corona}^{XRD} = \frac{v_{corona}^p}{\rho_{SiO2}(1-\varepsilon)\, v_{cell}^m} \qquad \text{Eq. SI-13}$$

These two specific volumes are found to be $V_{center}^{XRD}$ = 0.26 cm³ g$^{-1}$, and $V_{corona}^{XRD}$ = 0.23 cm³ g$^{-1}$. The sum of these two volumes is lower than the mesopore volume determined by physisorption. The total pore volume in the wall, is calculated as

$$V_{wall}^{XRD} = \frac{\varepsilon}{\rho_{SiO2}(1-\varepsilon)} \qquad \text{Eq. SI-14}$$

which leads to $V_{wall}^{XRD}$ = 0.19 cm³/g. This volume is 2 times larger than the microporous volume determined from physisorption.

Table SI-1 gathers the XRD and physisorption data of all samples analyzed in reference [21] and shows the calculated values of $\varepsilon$, $V_{center}^{XRD}$, $V_{corona}^{XRD}$ and $V_{wall}^{XRD}$, using Equations SI-11 to SI-14. The findings are the same as for the sample analyzed in the present paper: (i) the porosity of the wall is about 30%, (ii) the volume of the corona is much larger than the micropore volume, and (iii) the sum of center and corona pore volumes is lower than the mesopore volume, which means that the porosity of the wall is partly due to mesopores.

Table SI-1. Specific volumes of the samples of reference [21] derived from the linear corona modeling of XRD, and their comparison with physisorbed volumes.

| | $a$ (nm) | $r_i$ (nm) | $r_o$ (nm) | $V_{meso}^{N2}$ (cm³/g) | $V_{micro}^{N2}$ (cm³/g) | $\varepsilon$ (-) | $V_{center}^{XRD}$ (cm³/g) | $V_{corona}^{XRD}$ (cm³/g) | $V_{wall}^{XRD}$ (cm³/g) |
|---|---|---|---|---|---|---|---|---|---|
| P123AC | 9.6 | 2.4 | 4 | 0.6 | 0.1 | 0.33 | 0.26 | 0.21 | 0.22 |
| P123BC | 11.05 | 2.9 | 5.2 | 1.06 | 0 | 0.40 | 0.38 | 0.38 | 0.30 |
| P103AC | 8.8 | 1.9 | 3.8 | 0.52 | 0.12 | 0.31 | 0.19 | 0.25 | 0.21 |
| P103BC | 10.45 | 2.9 | 5.2 | 1.18 | 0 | 0.37 | 0.46 | 0.46 | 0.27 |

$a$: lattice spacing; $r_i$ and $r_o$: inner and outer radii of the corona ; $V_{meso}^{N2}$ and $V_{micro}^{N2}$: mesopore and micropore volumes; $\varepsilon$: porosity of the wall; $V_{center}^{XRD}$, $V_{corona}^{XRD}$ and $V_{wall}^{XRD}$: total pore volume located in the pore center and corona, and in the wall.